Combined Effect of Bond and Potential Disorder in Half-Doped Manganites

Sanjeev Kumar* and Arno P. Kampf

*Theoretical Physics III, Center for Electronic Correlations and Magnetism, Institute of Physics, University of Augsburg,
D-86135 Augsburg, Germany*
(Received 8 June 2007; published 22 February 2008)

We analyze the effects of both bond and potential disorder in the vicinity of a first-order metal insulator transition in a two-band model for manganites using a real-space Monte Carlo method. Our results reveal a novel charge-ordered state coexisting with spin-glass behavior. We provide the basis for understanding the phase diagrams of half-doped manganites, and contrast the effects of bond and potential disorder and the combination of both.

The perovskite manganites $R_{1-x}A'_x\text{MnO}_3$ ($R =$ rare earth, $A' =$ alkaline earth) have received attention from the condensed matter community, largely due to their colossal magnetoresistance (CMR) effect [1,2]. In these materials different ordering tendencies of charge, spin, lattice, and orbital degrees of freedom compete. Because of this complexity the understanding of the sensitive influence of quenched disorder has become one of the central issues in manganites' research. Based on a variety of experiments, Tomioka and Tokura have shown that the observed phases near half-doping can be organized in terms of two parameters: the average radius $r_A = (1 - x)r_R + xr_{A'}$ and the variance σ^2 of the ionic radii [3]. Since r_A and σ^2 control the single-particle bandwidth and the amount of disorder, respectively, quenched disorder is thereby identified as one key parameter in manganites. This is supported via a set of experiments on the ''ordered'' and ''disordered'' compositions of $R_{0.5}\text{Ba}_{0.5}\text{MnO}_3$, with a sequence of decreasing r_A as R ranges from La to Y [4,5]. The ground state for the ordered materials changes from a ferromagnetic metal (FM-M) to an A-type antiferromagnetic (AFM) insulator (I) near $R = \text{Pr}$, eventually followed by a charge and orbitally ordered insulator with ferromagnetically aligned spins along zigzag chains, which is commonly referred to as the CE phase [1]. In the disordered materials the AFM phase does not exist and the Curie temperature (T_C) is suppressed. A spin-glass (SG) phase is observed for R ranging from Sm to Dy. Disordered $\text{Nd}_{0.5}\text{Ba}_{0.5}\text{MnO}_3$ undergoes an insulator to metal transition near T_C, which is characteristic of CMR materials. On applying an external magnetic field, the spin-glass state can be driven towards a ferromagnetic metallic phase [6,7].

Theoretical studies of manganite-specific models at half-doping have indeed found a variety of ordered phases and transitions for clean systems [8,9]. Among them, the first-order phase transitions are particularly interesting, since these are assumed to split into two second-order transitions with an intermediate region of macroscopic phase coexistence upon including quenched disorder [1].

Detailed model studies to verify this assumption have only recently begun [10]. However, the modeling of disorder, which originates from different microscopic sources, has remained a matter of choice. Since the R or A' ions are located away from the electronically active Mn-O$_2$ planes, the primary effect of ionic-size mismatch is to modify the Mn-O-Mn bond angles [11,12]. A realistic model ansatz for disorder should necessarily account for these bond-angle variations. Additionally, the random positions of differently charged R^{3+} and Ba^{2+} ions results in an effective on-site disorder via Coulomb interactions. Therefore, both these sources of disorder are important and unavoidably occur together in doped manganites.

In this Letter, we provide a systematic analysis for the phase diagrams of $R_{0.5}\text{Ba}_{0.5}\text{MnO}_3$ by modeling the Mn-O-Mn bond-angle variations by angle dependent hopping parameters in a two-dimensional two-band double-exchange model with electron-lattice and electron-electron interactions. We use the combination of a real-space Monte Carlo method and an unrestricted Hartree-Fock scheme. Bond-disorder alone explains the suppression of the Curie temperature and the existence of a spin-glass phase, but its effect on the charge and orbital ordering is weak. Therefore, a phase is formed with coexisting charge and orbital order and glassiness in the spin degree of freedom. We identify a thermally driven metal to insulator transition, as well as a magnetic field driven spin-glass insulator to ferromagnetic metal transition. We find that disorder does not lead to macroscopic phase coexistence, but rather generates inhomogeneities on the scale of few lattice spacings.

Specifically, we choose a two-band model with quenched disorder for itinerant e_g electrons coupled to localized $S = 3/2$ t_{2g} spins and to the Jahn-Teller (JT) lattice distortions. The interorbital Hubbard repulsion U' between the e_g electrons and the AFM superexchange J_S between neighboring t_{2g} core spins are also included.

Based on the results of previous analyses [13], we adopt the double-exchange limit for the Hund's rule coupling, leading to the Hamiltonian:

$$H = \sum_{\langle ij \rangle}^{\alpha\beta} t_{ij}^{\alpha\beta} f_{ij} c_{i\alpha}^{\dagger} c_{j\beta} + \sum_i (\epsilon_i - \mu) n_i + J_S \sum_{\langle ij \rangle} \mathbf{S}_i \cdot \mathbf{S}_j$$

$$- \lambda \sum_i \mathbf{Q}_i \cdot \boldsymbol{\tau}_i + \frac{K}{2} \sum_i |\mathbf{Q}_i|^2 + U' \sum_i n_{ia} n_{ib}. \quad (1)$$

In Eq. (1), α, β are summed over the two Mn-e_g orbitals $d_{x^2-y^2}$ (a) and $d_{3z^2-r^2}$ (b). The operator $c_{i\alpha}$ ($c_{i\alpha}^{\dagger}$) annihilates (creates) an electron at site i in orbital α with its spin slaved along the direction of the t_{2g} spin $\mathbf{S}_i$. $t_{ij}^{\alpha\beta}$ denote the hopping matrix elements between e_g orbitals on nearest-neighbor Mn ions via the oxygen $2p$ orbitals, and hence depend on the Mn-O-Mn bond angle ϕ_{ij}. Taking into account the $pd\sigma$ contributions only, the hopping parameters between neighboring sites i and j are given by [14]

$$t_{ij}^{aa} = t\cos^3(\phi_{ij}); \quad t_{ij}^{bb} = (t/3)\cos(\phi_{ij});$$

$$t_{ij,x(y)}^{ab} \equiv t_{ij,x(y)}^{ba} = +(-)(t/\sqrt{3})\cos^2(\phi_{ij}). \quad (2)$$

Here, x and y denote the spatial directions on a square lattice and $t = 3/4(pd\sigma)^2$ is the basic energy unit. The factors $f_{ij} = \cos(\Theta_i/2)\cos(\Theta_j/2) + \sin(\Theta_i/2)\sin(\Theta_j/2) \times e^{-i(\Phi_i - \Phi_j)}$ are a consequence of projecting out fermions with spins antialigned to the core-spin directions. Θ_i and Φ_i are the polar and azimuthal angles determining the orientation of the t_{2g} spin $\mathbf{S}_i$.

Bond-disorder arises from a nonuniform distribution of the bond angles ϕ_{ij}; on-site disorder enters via the local potentials ϵ_i, for which equally probable values $\pm\Delta$ are assumed. λ denotes the strength of the JT coupling between the distortion $\mathbf{Q}_i = (Q_i^x, Q_i^z)$ and the orbital pseudo-spin $\tau_i^{\mu} = \sum_{\sigma}^{\alpha\beta} c_{i\alpha\sigma}^{\dagger} \Gamma_{\alpha\beta}^{\mu} c_{i\beta\sigma}$, where Γ^{μ} are the Pauli matrices [1]. The spins are treated as classical unit vectors, $|\mathbf{S}_i| = 1$, and the lattice variables are considered in the adiabatic limit. μ denotes the chemical potential and the lattice stiffness K is set to 1.

The average ionic radius r_A in $R_{0.5}Ba_{0.5}MnO_3$ is modeled by the average angle ϕ_0. The ordered compounds are represented by a uniform Mn-O-Mn angle $\phi_{ij} \equiv \phi_0$, and for the disordered systems the angles ϕ_{ij} are selected from a binary distribution with mean ϕ_0 and variance $\delta\phi$. Since the amount of disorder depends on the difference in ionic radii of R and Ba ions, ϕ_0 and $\delta\phi$ are not independent. This is reflected in the similar behavior of ordered and disordered $La_{0.5}Ba_{0.5}MnO_3$, due to the similar ionic radii of La and Ba [5]. We therefore set $\delta\phi = \phi_0^{La} - \phi_0$, where $\phi_0^{La} = 175°$ is the average bond angle in $La_{0.5}Ba_{0.5}MnO_3$ [15]. ϕ_0 is assumed to decrease from 175° to 164°, as R changes from La to Y. Our parameter choice, $\lambda = 1.4$, $U' = 6$, and $J_S = 0.08$ is guided by the observed scales for the Néel temperature in $CaMnO_3$ and the transport gap in $LaMnO_3$ [16,17].

Certain limits of the model Hamiltonian Eq. (1) have been analyzed already. The effects of large U' have been addressed within mean-field theories for a restricted choice of magnetic phases [18,19]. In the absence of the Hubbard

term, various ordered phases were discovered at half-doping using an exact diagonalization (ED) based Monte Carlo method [8]. The effect of on-site disorder near a first-order phase boundary was reported recently [10]. But a realistic and simultaneous treatment of bond and potential disorder and the explicit treatment of an interorbital Hubbard term, while exactly retaining the spatial correlations, have so far been lacking.

Here, we use a combination of the unrestricted Hartree-Fock (HF) scheme and the traveling cluster approximation (TCA). The TCA allows for sampling of classical configurations for spin and lattice variables according to the Boltzmann weight, and involves iterative ED of small clusters [20]. The Hartree-Fock decomposition of the Hubbard term leads to three independent HF parameters per site $\langle n_{ia} \rangle$, $\langle n_{ib} \rangle$, and $\langle \tau_i^+ \rangle = \langle c_{ib}^{\dagger} c_{ia} \rangle$, which enter as additional parameters in TCA. These HF parameters are self-consistently evaluated with the annealing process of the TCA. Most results are on lattices with $N = 16^2$ sites using a traveling cluster with $N_c = 4^2$.

The indicators for spin- and charge ordering are plotted in Fig. 1. Figure 1(a) shows the temperature dependent magnetization, defined via $m^2 = \langle (N^{-1} \sum_i \mathbf{S}_i)^2 \rangle_{av}$, for clean and bond-disordered systems for $\phi_0 = 170°$. Here and below $\langle \ldots \rangle_{av}$ denotes the average over thermal equilibrium configurations, and additionally over realizations of quenched disorder. Bond disorder with $\delta\phi = 5°$ considerably reduces the Curie temperature T_C, which is estimated from the inflection point in $m(T)$. Recall that the strength of bond disorder $\delta\phi$ is tied to the average bond angle ϕ_0 via $\delta\phi = \phi_0^{La} - \phi_0$. In the clean system $m(T)$ and, in particular, T_C are not affected much upon
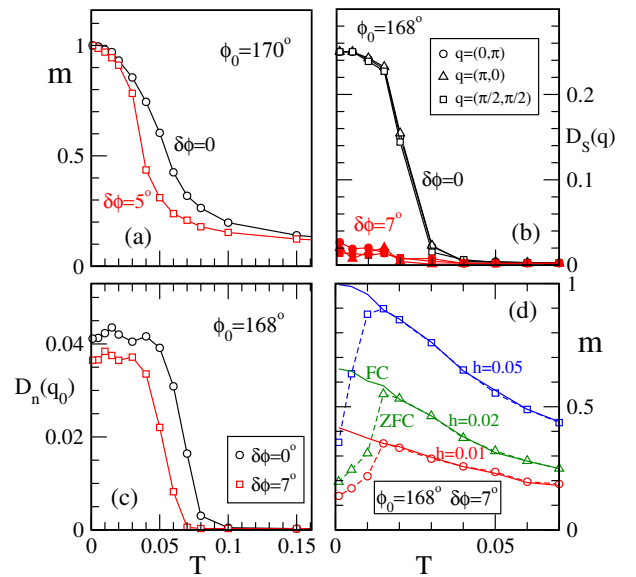

FIG. 1 (color online). Temperature dependence of (a) the magnetization, (b) the spin structure factor at selected momenta, and (c) the staggered charge structure factor for clean and bond-disordered systems. (d) Field-cooled (FC) and zero-FC magnetization for the bond-disordered system.

varying ϕ_0. The fingerprint of CE spin order is the simultaneous presence of peaks at wave vectors $\mathbf{q} = (0, \pi)$, $(\pi, 0)$, and $(\pi/2, \pi/2)$, in the spin structure factor $D_S(\mathbf{q}) = N^{-2} \sum_{ij} \langle \mathbf{S}_i \cdot \mathbf{S}_j \rangle_{av} \, e^{-i\mathbf{q} \cdot (\mathbf{r}_i - \mathbf{r}_j)}$. In Fig. 1(b), a simultaneous rise in the three components of $D_S(\mathbf{q})$ is observed for $\delta\phi = 0°$, whereas in the disordered case no sizable peaks appear at any $\mathbf{q}$.

For the clean system, the charge structure factor $D_n(\mathbf{q}) = N^{-2} \sum_{ij} \langle n_i \cdot n_j \rangle_{av} \, e^{-i\mathbf{q} \cdot (\mathbf{r}_i - \mathbf{r}_j)}$ at $\mathbf{q} = \mathbf{q}_0 \equiv (\pi, \pi)$ rises sharply upon cooling [see Fig. 1(c)], indicating the onset of staggered charge order. The temperature scales T_{CO} and T_{CE} are inferred from inflection points in the T dependence of the relevant components of the charge and spin structure factors. Charge ordering is accompanied by the ordering of lattice and orbital variables. The U' term enhances T_{CO}, which is otherwise of the same order as T_{CE} for the values of λ used here [9]. Surprisingly, a clean signal for the onset of charge ordering near $T \sim 0.06$ is found even in the bond-disordered system. This highlights the crucial qualitative difference between the effects of bond and on-site disorder. The latter is known to strongly suppress charge ordering tendencies [21]. Upon comparing Figs. 1(b) and 1(c), it becomes clear that the bond disorder leads to a state that is ordered in the orbital and the charge sector but disordered in the spin sector. The U' term further stabilizes the charge order in this state.

Additional information about the spin state that emerges in the presence of bond disorder is obtained from the field-cooled (FC) and zero-field-cooled (ZFC) magnetizations, which we calculate by including a Zeeman term $-h\sum_i S_i^z$, in the Hamiltonian. While the FC and ZFC magnetizations are indistinguishable for a clean system, their difference at low T may serve as an indicator for a spin-glass character for a bond-disordered system [see Fig. 1(d)] [22]. The temperature for which the FC and ZFC results begin to differ provides an estimate for the spin-glass crossover temperature T_g. Such a state with charge and orbital order but glassiness in the spin sector was recently reported for single-layered manganites [23].

Figure 2(a) shows the phase diagram in the $T - \phi_0$ plane, for the clean system. For $\phi_0 \gtrsim 170°$, the system undergoes a paramagnet (PM) to ferromagnet transition upon cooling. For $\phi_0 \lesssim 169°$, charge and orbital degrees of freedom order at low temperatures, followed by a transition from a PM to a CE spin state near $T \sim 0.02$. The ϕ_0-driven transition at low T results from the reduction in bandwidth upon decreasing ϕ_0. Thereby the effective λ and J_S are enhanced leading to a first-order transition towards a charge and orbital ordered (CO-OO) CE state by opening a gap in the spectrum, at a critical value ϕ_0^C. ϕ_0^C increases from 155° for $U' = 0$ to 169° for $U' = 6$. While charge and orbital order is only weakly affected by bond disorder, the spin degree of freedom reacts more sensitively [see Fig. 2(b)]. For $\phi_0 \lesssim 169°$, glassiness in the spin sector is induced [see Fig. 1(d)], and for $172° \gtrsim \phi_0 \gtrsim 170°$, T_C is strongly suppressed.

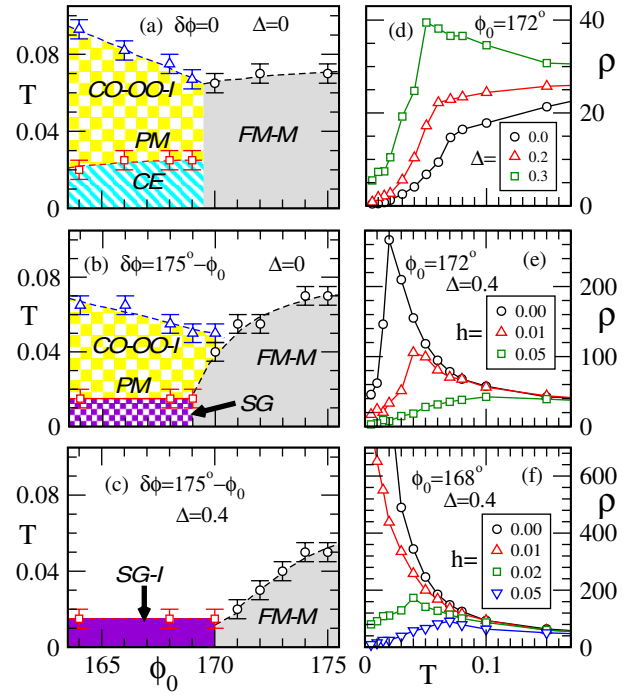FIG. 2 (color online). $T - \phi_0$ phase diagrams at $\lambda = 1.4$, $J_S = 0.08$, and $U' = 6$, (a) $\delta\phi = 0°$, $\Delta = 0$, (b) $\delta\phi = 175° - \phi_0$, $\Delta = 0$, and (c) $\delta\phi = 175° - \phi_0$, $\Delta = 0.4$. Symbols are data points and dotted lines are guides to the eye. FM (PM) denotes a ferromagnetic (paramagnetic) state; M (I) indicates metallic (insulating) character; CO (OO) refers to charge (orbital) order; and SG marks the spin-glass state. (d) T-dependent resistivity ρ for increasing strength of on-site disorder, in units of $\hbar/\pi e^2$. $\rho(T)$ for varying magnetic field for $\Delta = 0.4$, and (e) $\phi_0 = 172°$, (f) $\phi_0 = 168°$.

Some of the key features of the experimental phase diagram for the disordered materials are not captured by bond disorder alone; i.e., there is no charge disordered SG state and a FM-M to PM-I transition exists only in a very narrow ϕ_0 window. Therefore, we include additional on-site disorder. Charge order is lost for finite on-site disorder, while the spin-glass phase persists [see Fig. 2(c)]. The ground state becomes an unsaturated FM for $170° > \phi_0 > 173°$ and T_C is further reduced. The phase diagram in Fig. 2(c) compares very well with the experimental phase diagram of half-doped manganites [5].

Figure 2(d) shows the effect of on-site disorder on the resistivity ρ of a bond-disordered system with a ferromagnetic metallic ground state. ρ is approximated by the inverse of $\sigma(\omega_{min})$, where $\omega_{min} = 10t/N \sim 0.04t$ is the lowest reliable energy scale for calculations of the optical conductivity $\sigma(\omega)$ on our 16^2 system [24]. Insulating or metallic character is determined from the sign of the slope of $\rho(T)$. Increasing the strength Δ of the on-site disorder leads to a reduction in T_C and an increase in the resistivity, and an FM-M to PM-I transition is observed for $\Delta = 0.3$.

If the ground state is ferromagnetic, the resistivity in an external field drops near T_C [see Fig. 2(e)], similar to the experiments in $Nd_{0.5}Ba_{0.5}MnO_3$. A magnetic field reduces
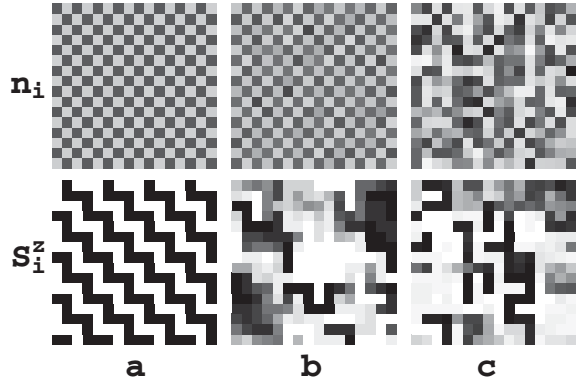
FIG. 3. Monte Carlo snapshots for $\phi_0 = 168°$ on a 16×16 lattice. Column (a): $\delta\phi = 0°$, $\Delta = 0$; column (b): $\delta\phi = 7°$, $\Delta = 0$; and column (c): $\delta\phi = 0°$, $\Delta = 0.4$. The top row shows the charge density n_i, grayscale covering the range from 0.2 (white) to 0.8 (black). The bottom row plots the spin component S_i^z, grayscale from -1 (white) to 1 (black). Results are shown for specific realizations of disorder at $T = 0.005$.

the resistivity in the SG phase at low T; additionally $d\rho/dT$ changes sign, indicating an insulator to metal transition [see Fig. 2(f)]. Such transitions are indeed observed in $(Sm_{0.3}Gd_{0.7})_{0.55}Sr_{0.45}MnO_3$ [6,7].

Figure 3 shows real-space patterns for the charge n_i and the spin S_i^z variables for clean (column a), bond-disordered (column b), and on-site disordered (column c) systems. The ground state in the clean case is a CE phase with charge and orbital order. A checkerboard pattern for the charge density and a zigzag FM chain structure for spin variables characterize this phase [8]. Bond disorder does not affect the charge ordering, while the spins **S** become disordered leading to a nontrivial state with simultaneous charge order and spin glassiness. On-site disorder spoils the charge ordering and the magnetic order. The spatial patterns reveal inhomogeneities on the scale of a few lattice spacings. Since charge order can exist in the PM phase at elevated temperatures [see Figs. 2(a) and 2(b)], its coexistence with spin-glass behavior is not surprising. The different effects of bond disorder on charge and spin degrees of freedom is, however, nontrivial. On the one hand, a decreasing bond angle leads to a lowering of the fermionic kinetic energy across that bond and thereby reduces the tendency towards double-exchange ferromagnetism. But more importantly, the zigzag structure of the spin-aligned chains in the CE phase is disrupted by random weak bonds. The charge variables instead vary only weakly with bond disorder, which explains the stability of the charge-ordered state.

In summary, a two-band double-exchange model with electron-lattice and electron-electron interactions with bond and on-site disorder provides the basis for an overall understanding of the experimental phase diagram of $R_{0.5}Ba_{0.5}MnO_3$ [5]. Our results reveal the existence of a

nontrivial phase, which is ordered in the charge variables but glassy in the spin variables. The bond disorder is important for the spin-glass behavior, and is likely to explain the coexistence of charge order and spin glassiness in single-layered manganites [23]. On-site disorder is crucial for a description of the thermally driven metal to insulator transitions. Each of the two types of disorder explain selected features in manganites, but only a combination of both can describe most of the experimentally observed phenomena.

*Present address: Faculty of Science and Technology, University of Twente, P.O. Box 217, 7500 AE Enschede, The Netherlands.

[1] For overviews see *Nanoscale Phase Separation and Colossal Magnetoresistance*, edited by E. Dagotto (Springer-Verlag, Berlin, 2002), and [2].

[2] *Colossal Magnetoresistive Oxides*, edited by T. Chatterji (Kluwer Academic Publishers, Dordrecht, 2004).

[3] Y. Tomioka and Y. Tokura, Phys. Rev. B **70**, 014432 (2004).

[4] "Ordered" refers to the replacement of rare-earth ions by Ba in an entire layer, while "disordered" means a solid solution of $R_{0.5}Ba_{0.5}MnO_3$ as discussed in [5].

[5] D. Akahoshi *et al.*, Phys. Rev. Lett. **90**, 177203 (2003).

[6] Y. Tomioka *et al.*, Phys. Rev. B **68**, 094417 (2003).

[7] A. Maignan *et al.*, Phys. Rev. B **60**, 15214 (1999).

[8] S. Yunoki *et al.*, Phys. Rev. Lett. **84**, 3714 (2000).

[9] L. Brey, Phys. Rev. B **71**, 174426 (2005).

[10] C. Sen *et al.*, Phys. Rev. Lett. **98**, 127202 (2007).

[11] L. M. Rodriguez-Martinez and J. P. Attfield, Phys. Rev. B **58**, 2426 (1998).

[12] J. Fontcuberta *et al.*, Phys. Rev. Lett. **76**, 1122 (1996).

[13] Hund's rule coupling is known to be large (~1 eV) in manganites, and the essential physics is retained in the double-exchange limit $J_H \rightarrow \infty$. See, e.g., E. Dagotto *et al.*, Phys. Rep. **344**, 1 (2001).

[14] J. C. Slater and G. F. Koster, Phys. Rev. **94**, 1498 (1954).

[15] O. Chmaissem *et al.*, Phys. Rev. B **64**, 134412 (2001).

[16] Z. Jirak *et al.*, J. Magn. Magn. Mater. **53**, 153 (1985).

[17] T. T. M. Palstra *et al.*, Phys. Rev. B **56**, 5104 (1997).

[18] R. Maezono *et al.*, Phys. Rev. B **58**, 11583 (1998).

[19] S. K. Mishra *et al.*, Phys. Rev. B **56**, 2316 (1997).

[20] S. Kumar and P. Majumdar, Eur. Phys. J. B **50**, 571 (2006).

[21] Y. Motome *et al.*, Phys. Rev. Lett. **91**, 167204 (2003); C. Sen *et al.*, Phys. Rev. B **70**, 064428 (2004).

[22] The confirmation of a spin-glass phase requires access to the spin dynamics. This, however, is beyond the scope of the present study, and we therefore take the difference between FC and ZFC magnetizations as our working definition for the spin-glass state.

[23] R. Mathieu *et al.*, Europhys. Lett. **80**, 37001 (2007).

[24] S. Kumar and P. Majumdar, Eur. Phys. J. B **46**, 237 (2005).